

Mirror-mode storms inside stream interaction regions and in the ambient solar wind: A kinetic study

O. Enríquez-Rivera,¹ X. Blanco-Cano,¹ C. T. Russell,² L. K. Jian,^{3,4} J. G. Luhmann,⁵ K. D. C Simunac,⁶ and A. B. Galvin⁶

Received 26 August 2012; revised 11 November 2012; accepted 20 November 2012; published 27 January 2013.

[1] Mirror-mode structures have been found in the solar wind at various heliocentric distances with different missions. Recently, STEREO has observed mirror-mode waves present as trains of holes and also as humps in the magnetic field magnitude. In some cases, mirror-mode trains last for very long periods of time and have been called “mirror-mode storms”. We present case studies of mirror-mode storms observed in the solar wind using STEREO data in three different locations: in the downstream region of the forward shock of a stream interaction region, inside a stream interaction region far from the forward shock, and also in the ambient solar wind. To make a formal identification of the mirror mode, we determine wave characteristics using minimum variance analysis. Finally, we perform a kinetic dispersion analysis and discuss the possible origin of mirror-mode structures evaluating curves of growth for different regimes of proton temperature anisotropies in a plasma with a He component.

Citation: Enríquez-Rivera, O., X. Blanco-Cano, C. T. Russell, L. K. Jian, J. G. Luhmann, K. D. C Simunac, and A. B. Galvin (2013), Mirror-mode storms inside stream interaction regions and in the ambient solar wind: A kinetic study, *J. Geophys. Res. Space Physics*, 118, 17–28, doi:10.1029/2012JA018233.

1. Introduction

[2] The mirror-mode instability is a fundamental plasma instability that leads to compressional nonpropagating (zero real frequency in the plasma rest frame) magnetic field fluctuations [Hasegawa, 1969]. Such fluctuations are linearly polarized waves that grow preferentially in directions oblique to the background magnetic field. A typical signature of mirror-mode structures is the anticorrelation between the magnetic field strength and density fluctuations, a feature that is also observed for the slow-mode waves.

[3] The mirror mode can be treated using a fluid approximation. However, it has been noted that a kinetic treatment is more appropriate [Tajiri, 1967; Hasegawa, 1969; Southwood and Kivelson, 1993; Krauss-Varban *et al.*, 1994; Génot *et al.*, 2001] because the physics of the mirror

instability involves nonfluid processes (i.e., wave-particle resonances), which play an important role in hot plasmas.

[4] In the low-frequency range (below the ion-cyclotron frequency), plasmas in which the perpendicular temperature T_{\perp} is larger than the parallel temperature T_{\parallel} behave in such a way that the perpendicular pressure δp_{\perp} responds to a compressional change in the magnetic field strength δB in anti-phase [Hasegawa, 1969]. In other words,

$$\delta p_{\perp} = 2p_{\perp} \left(1 - \frac{T_{\perp}}{T_{\parallel}}\right) \frac{\delta B}{B} \quad (1)$$

[5] In a bi-Maxwellian plasma, equation (1) leads to the following condition (for more details see Southwood and Kivelson [1993]):

$$1 + \beta_{\perp} \left(1 - \frac{T_{\perp}}{T_{\parallel}}\right) < 0 \quad (2)$$

where β stands for the ratio of plasma thermal to magnetic pressure. Equation (2) is the well-known mirror instability criterion and is satisfied either with high values of β or high temperature anisotropies (T_{\perp}/T_{\parallel}).

[6] Linear Vlasov theory predicts that for high-temperature anisotropies, the ion-cyclotron instability can also grow from the free energy available in such an anisotropy usually dominating over the mirror mode [Gary, 1992]. Nevertheless, in situ observations of mirror-mode waves in thermally anisotropic space plasmas are very frequent [Winterhalter *et al.*, 1994; Liu *et al.*, 2006; Génot *et al.*, 2009]. Space plasma environments where nonuniform heating and compression take place, such as the downstream regions of shocks, are excellent sources for temperature anisotropies

¹Instituto de Geofísica, Universidad Nacional Autónoma de México, Coyoacán D.F., Mexico.

²University of California, Los Angeles, Institute of Geophysics and Planetary Physics, Los Angeles, California, USA.

³University of Maryland, College Park, Maryland, USA.

⁴NASA Goddard Space Flight Center, Greenbelt, Maryland, USA.

⁵Space Science Laboratory, University of California, Berkeley, California, USA.

⁶Space Science Center, University of New Hampshire, Durham, New Hampshire, USA.

Corresponding author: O. Enríquez-Rivera, Instituto de Geofísica, Universidad Nacional Autónoma de México, Coyoacán, D.F., 04510, Mexico. (oenriquez@geofisica.unam.mx)

in the plasma. Ion pick up processes can favor the existence of temperature anisotropies as well. The fact that mirror-mode waves have been observed in such environments with and without the presence of ion-cyclotron waves is still an issue of study. It has been suggested, for instance, that the addition of a helium component can suppress the growth rate for ion-cyclotron waves [Price *et al.*, 1986; Gary, 1993] and favor the growth of mirror modes. Likewise, inhomogeneities created in the background plasma by mirror modes can inhibit the growth of ion-cyclotron waves [Southwood and Kivelson, 1993].

[7] The morphology of mirror-mode structures has been a long standing issue. Observations of mirror-mode structures throughout the heliosphere have taught us that the morphology of mirror-mode waves is diverse. Magnetic field enhancements (peaks) and depressions (holes) are the most common signatures of the mirror mode, the latter feature being more frequently observed. In planetary magnetosheaths such as Earth, Saturn, and Jupiter, trains of peaks are observed very often near the planet’s bow shock and in the middle magnetosheath, while trains of holes have a tendency to appear closer to the magnetopause and on the flanks [Bavassano Cattaneo *et al.*, 1998; Lucek *et al.*, 1999; Joy *et al.*, 2006; Génot *et al.*, 2001, 2009]. In Saturn’s case, mirror modes may also appear as quasi-sinusoidal structures, which evolve into holes and peaks near the magnetopause [Bavassano Cattaneo *et al.*, 1998]. Trains of magnetic holes and peaks have been also observed in the heliosheath and interpreted as mirror-mode structures [Burlaga *et al.*, 2006]. Similarly, Liu *et al.* [2006] found magnetic field holes ahead of interplanetary coronal mass ejections.

[8] For the solar wind, magnetic holes have also been observed at various heliocentric distances either as isolated holes or trains of closely-spaced magnetic holes [Winterhalter *et al.*, 1994; Zhang *et al.*, 2008; Russell *et al.*, 2008]. Recently, using STEREO high-resolution magnetic field data, Russell *et al.* [2009] reported several mirror-mode events of small amplitude trains, which included not only holes, but also peaks that persisted for hours and were referred to as “mirror-mode storms”. Such events were found in moderate-high β solar wind or downstream of weak interplanetary shocks.

[9] There is evidence that mirror modes have important effects on energetic particle diffusion [Tsurutani *et al.*, 1999] and electron thermal conductivity [Schekochihin *et al.*, 2008]. What is more, it has also been suggested that mirror modes observed at 1 AU might even be an indicator of the presence of ion-cyclotron waves in the solar corona [Russell *et al.*, 2008]. The fact that the mirror mode is a commonly observed fundamental plasma instability in the heliosphere and that it plays important roles in the above mentioned phenomena makes the study of mirror modes of interest itself. Nevertheless, mirror-mode properties (i.e., size, shape, and orientation) are poorly known. Furthermore, their origin and evolution are still discussed and remain mysterious. In this work we use STEREO data to study in detail mirror modes present as “mirror-mode storms” (MMS) in the solar wind. This work is meant to gain insight into the study of mirror-mode characteristics and its origin.

[10] Unlike mirror modes observed in the magnetosheath of planetary shocks, the properties of mirror-mode structures

observed near interplanetary shocks (IP) have been less studied. Tsurutani *et al.* [1992] interpreted a series of magnetic dips observed by Ulysses in the plasma behind an IP shock associated with an Interplanetary Coronal Mass Ejection (ICME) as being caused by the mirror instability. More recently, Liu *et al.* [2006] investigated the presence of mirror modes in the sheath regions between fast interplanetary coronal mass ejections and their preceding shocks. An earlier work by Winterhalter *et al.* [1994] reported an event of magnetic holes observed by Ulysses in a region of plasma with $T_{\perp} > T_{\parallel}$ extending around 4 h downstream of a strong reverse shock. In that work, the authors made a statistical study and found several mirror mode holes present in interaction regions and other cases associated to plasma originating in coronal mass ejections. Similarly, Russell *et al.* [2009] reported two events where “mirror-mode storms” are observed downstream of weak interplanetary shocks associated with the leading edge of stream interactions. From these works, it seems that mirror-mode structures tend to occur in regions where fast streams reach slower solar wind. Our goal in this work is to further analyze the relationship between mirror modes (i.e., mirror-mode storms) and stream interaction region’s (SIR) IP shocks. Until now, the microphysics of plasma regions associated to macrostructures such as SIRs has not been studied in detail. The fact that mirror-mode storms are present inside such regions provides us an excellent opportunity to explore microstructures within SIRs.

[11] We analyzed 15 months of STEREO magnetic field data from January 2007 to March 2008, and present two case studies of mirror-mode storms inside SIRs and one case study of a mirror-mode storm embedded in ambient solar wind. We mainly concentrate on the microstructure of the plasma where mirror-mode storms were observed. This study is also intended to give an update of mirror-mode storms observed by STEREO and to contribute to the study of mirror-mode storms, which have been recently discovered and are yet poorly understood.

[12] The outline of this paper is as follows. In section 2, we describe the method used for the identification of mirror-mode storms observed by STEREO. In section 3, we show case studies of mirror modes found inside SIRs and in the ambient solar wind. Section 4 is devoted to kinetic dispersion analysis; here we explore the possibility that regions inside SIRs might provide the necessary plasma conditions (high-moderate betas, high-temperature anisotropies, and alpha particle density enhancements) for the growth of mirror-mode storms. Our main results are discussed and summarized in the final section.

2. Stereo Observations

2.1. Data and Mirror Mode Identification

[13] We surveyed mirror-mode storms (MMSs) observed by the STEREO mission during 2007 and January to March 2008. We used magnetic field data from the STEREO magnetometer and plasma data from the PLASTIC ion spectrometer [Galvin *et al.*, 2008]. The sampling frequencies are 8 Hz for magnetic field data and one sample per minute for plasma data.

[14] Figure 1 shows an example of a mirror-mode storm event observed on 10 July 2007 by STEREO B. Here, the mirror-mode storm can be recognized by the train of

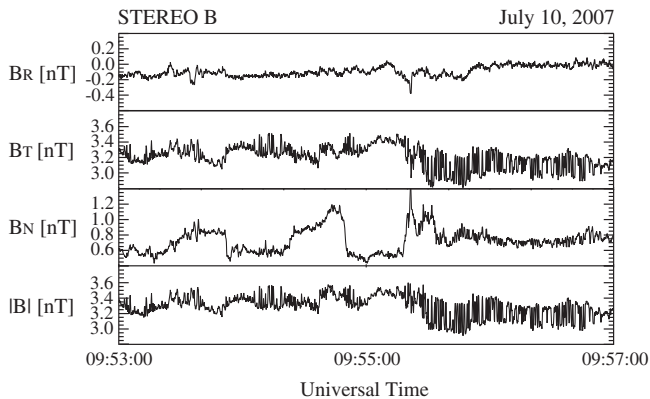


Figure 1. Magnetic field data of a mirror mode storm observed downstream of a forward shock associated with a SIR. Data are displayed in RTN coordinates.

compressive fluctuations shaped as peaks and holes that are clearly seen in the B magnitude and in the B_T component. The first storm was observed to start at 09:53 and the last storm episode continued until 17:30. In this case, the storms were observed in the leading edge of a SIR detected on 10 July 2007 at 09:45. When observed in great detail (see subsequent figures), MMSs resemble mirror-mode trains reported in previous works of mirror modes in the solar wind (see for instance, *Zhang et al.* [2008], and references therein). However, there are certain features that, to the naked eye, make them different from ordinary trains. First, the length of mirror-mode storms is usually longer than in the wave train reported in previous works. Second, the proximity between mirror-mode structures is shorter in mirror-mode storms. Based on these characteristics, we developed criteria to discriminate between ordinary trains of mirror modes and mirror-mode storms in our observations.

[15] There are several definitions of mirror-mode trains. Our definition of a mirror-mode train follows *Zhang et al.*'s [2008] criteria, which states that a train of mirror-mode holes (or also peaks in this case) is defined if there is at least a second comparable magnetic hole (peak) in a 5 min interval. On the other hand, we define a “mirror-mode storm” as a mirror-mode train that occurs in an interval that lasts at least 5 min as long as there are two dips or peaks in 40 s sliding windows. This last requirement guarantees the presence of a sufficient number of mirror-mode elements within a small interval for an event to be considered a mirror-mode storm. This number was obtained empirically after looking carefully at all the events used in this work and those reported in *Russell et al.* [2009].

[16] The method used in this work for the detection of mirror-mode structures in the magnetic field data is the following. First, we scanned magnetic field data from STEREO A and B using 600 s windows making a visual inspection to select unambiguous events where local magnetic field depressions (holes) or magnetic field humps (peaks) were embedded in a relatively steady ambient magnetic field. Using this method, we found hundreds of isolated structures (holes) as well as some events of mirror-mode trains. Because this work focuses on MMSs, we examined the total length of the mirror-mode trains and the proximity between the structures to evaluate if the structures met the above-mentioned criteria to be considered a mirror-mode storm.

[17] Mirror-mode waves are best identified by the anticorrelation between the magnetic field and the plasma density, as well as by the instability criterion given in equation (2). Unfortunately, the plasma resolution does not allow us to observe such anticorrelation; also, proton temperature anisotropy values are not yet available from the data to test the mirror instability criterion in our events. Alternatively, linear theory states that mirror-mode waves are compressive linearly polarized structures in the direction of B_0 . Thus, the second step in our mirror-mode identification method involves the study of wave polarization. To study wave polarization, we applied Minimum Variance Analysis (MVA) [*Sonnerup and Scheible*, 1998]. There are several criteria for identifying linearly polarized waves using MVA eigenvalues ratios [*Tátrallyay and Erdős*, 2005; *Génot et al.*, 2009, and references therein]. In this work we use criteria adapted from *Tátrallyay and Erdős* [2005]. For the observed structures to be considered linearly polarized waves, we require $\lambda_{\max}/\lambda_{\text{int}} > 2.5$ where λ_{\max} and λ_{int} are the maximum and intermediate eigenvalues of the covariance matrix, respectively. When applying the above criteria we found some events where this condition was not fulfilled because the waves were rather elliptic. This situation is in accordance with previous works [*Génot et al.*, 2001, 2009], where it has been noted that mirror-mode structures are more often observed as elliptic polarized waves. Thus, we relaxed the eigenvalue condition and cases where $1 < \lambda_{\max}/\lambda_{\text{int}} < \lambda_{\text{int}}/\lambda_{\min}$ and $\lambda_{\text{int}}/\lambda_{\min} > 3$ were considered elliptically polarized mirror-mode waves.

[18] Finally, we examined the angle between the maximum eigenvector and the mean magnetic field $\theta_{\max B_0}$. Because mirror-mode fluctuations are nearly parallel to B_0 , the condition $\theta_{\max B_0} < 20^\circ$ is required.

[19] Using the above method, we found that during 2007 and the first trimester of 2008, STEREO observed 14 events of mirror-mode storms inside SIRs. There are SIRs with more than one MMS, and the mission observed a total number of 40 SIRs during the period of study. We also found one case of a mirror-mode storm embedded in ambient solar wind, as well as MMSs associated to ICMEs. We reserve for a future paper the study of MMSs inside ICMEs.

3. Case Studies

3.1. Case Study 1: MMS Inside SIR Close to Forward Shock

[20] We have found that mirror-mode storms are very frequent in the downstream region of forward shocks of SIRs. Figure 2 shows magnetic field and plasma measurements of a SIR observed by STEREO A from 29 February to 3 March 2008. The shaded area just downstream from the forward shock indicates the period where mirror-mode structures were observed as mirror-mode storms. SIR time periods in this work are taken from the event lists available at the STEREO webpage from the University of California, Los Angeles (for more details see *Jian et al.* [2006]).

[21] Mirror-mode storm observations began on 29 February 2008 at 22:52:03, soon after the passage of the forward shock registered at 22:51:02. Figure 3 shows magnetic field data with a close-up of the interplanetary shock. The shock is quasi-perpendicular with $\theta_{Bn} = 84^\circ$ and has a magnetosonic

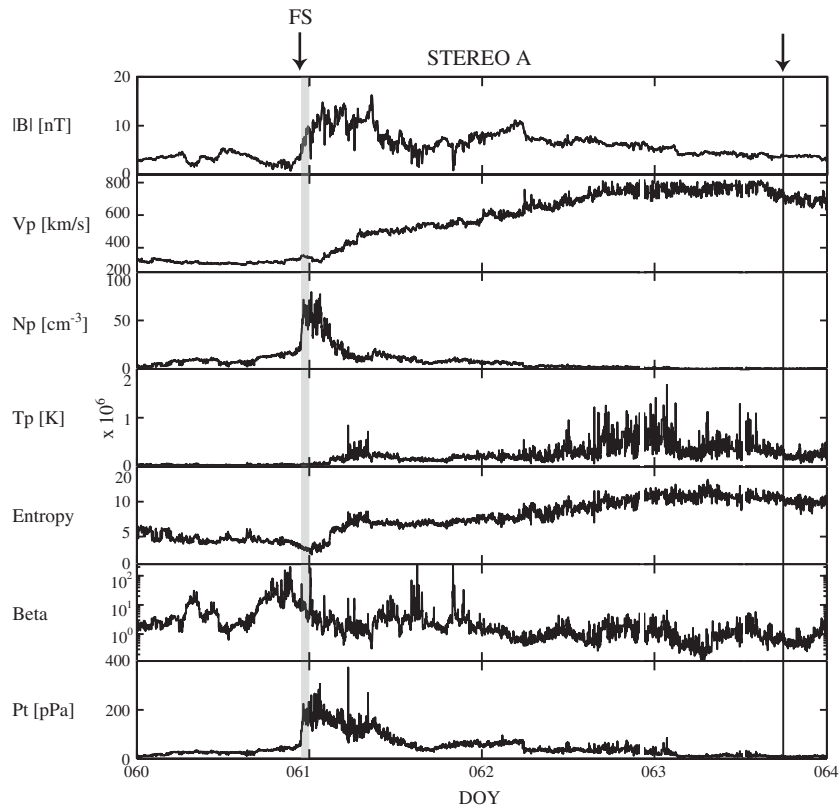


Figure 2. SIR observed on 29 February 2008 (edges of SIR are indicated with arrows). Mirror mode storms (shaded area) were observed downstream of the SIR’s forward shock.

Mach number of 1.3. As noted in Figure 3, whistler waves are observed downstream from the shock for less than 1 min and are soon replaced by the mirror-mode waves. The occurrence of mirror-mode structures ceased after 23:30. Figure 4 shows the evolution of the mirror-mode structures in intervals of 40 s during the storm. At the very beginning of the event, near the shock, mirror-mode waves are mainly small amplitude “peaks” (top of Figure 4A). A few minutes later, the number of peaks increases, and the time separation between them decreases (Figures 4B–4C). As time passes, holes begin to be detected, making it difficult to distinguish between peaks and holes (Figure 4D). Near the end of the storm event, the structures turn into nicely shaped holes which are deeper, wider, and more separated as the end of the event is approached (Figures 4F–4G). The normalized amplitudes ($\delta B/B_0$) of such holes can reach $\delta B/B_0 = 0.95$ approximately as seen in the hole presented in case G of Figure 4. During the MMS, the mean value of beta was 11.48 with a maximum peak of 51.59.

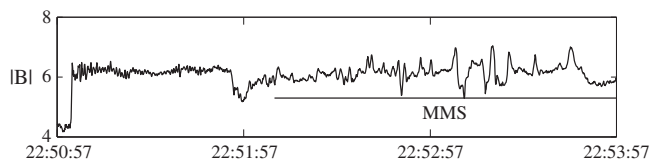


Figure 3. Magnetic field strength observed by STEREO A on 29 February 2008. Downstream of the forward shock registered at 22:51:02 an MMS was detected starting at 22:52:03.

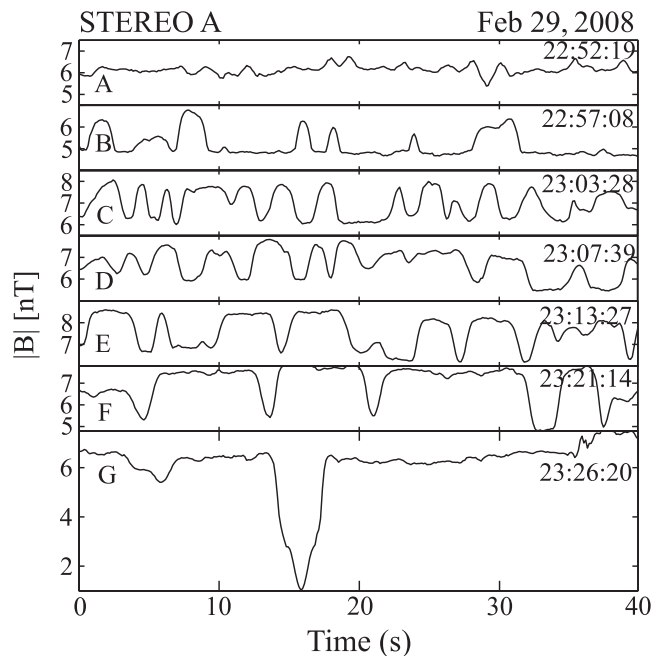


Figure 4. Forty seconds segments of B showing the development of magnetic structures during mirror mode storms observed on 29 February 2008. The starting time (HH:MM:SS) of each segment is indicated on the right hand side.

Table 1. Mirror Mode Storm Events Observed by STEREO During 2007 and the First Trimester of 2008

Event	Month	Day	Year	SPC	Mean Beta	MMS duration (min)	Structure	IP shock	Distance from SIR Leading Edge (km)	Na_2/Na_1	Na/Np
1	February	25	2007	SA	31.5	33.0	SIR	N		1.6	0.006
2	February	25	2007	SA	32.7	52.0	SIR	N		1.2	0.007
3	June	28	2007	SB	6.2	9.0	Ambient sw	N	Ambient sw	1.2	0.017
4	June	29	2007	SA	4.4	20.0	SIR	N	$2.65E+06$	5.6	0.009
5	June	29	2007	SA	4.7	41.0	SIR	N	$9.97E+06$	0.6	0.007
6	June	30	2007	SA	4.8	10.0	SIR	N	$2.25E+07$	2.7	0.011
7	July	3	2007	SB	3.3	26.0	SIR	N	$7.60E+05$	1.5	0.015
8	July	10	2007	SB	9.9	480.0	SIR	N	$1.88E+05$	1.6	0.006
9	August	14	2007	SB	2.4	13.0	SIR	N	$7.01E+05$	1.2	0.009
10	September	26	2007	SB	7.5	31.0	SIR	N	$1.66E+05$	5.2	0.025
11	October	18	2007	SA	16.2	9.0	SIR	Y	$1.30E+06$	0.9	0.004
12	December	8	2007	SB	3.4	7.0	SIR	Y	$1.14E+05$	no data	no data
13	December	16	2007	SB	3	9.0	SIR	Y	$0.00E+00$	no data	no data
14	January	29	2008	SB	4	27.0	SIR	Y	$1.10E+05$	no data	no data
15	February	29	2008	SA	11.5	38.0	SIR	Y	$2.08E+04$	1.4	0.002

[22] High-resolution (one sample per minute) alpha particle data (He^{++}) were used to study helium content in our mirror-mode events. On 29 February 2008, the value of alpha particle density (Na) increased from 0.082 cm^{-3} before the storm to 0.1124 cm^{-3} during the storm, which is an increase of almost 40%. To study Na enhancements in our MMS events, we calculated the parameter Na_2/Na_1 , which stands for the ratio between the mean value inside the storm (denoted by Na_2) and the mean value of Na before the storm occurs (denoted by Na_1), see Table 1. We also show in Table 1 the mean value of the parameter Na/Np during the storm, where Np is the proton density. For case study 1 (29 February 2008) $Na/Np=0.0024$.

[23] It is interesting to observe helium density enhancements in regions where mirror-mode structures are observed. As noted in earlier works [Gary *et al.*, 1976] plasmas where β is high ($\beta > 1$) and temperature anisotropies are moderate

or even high (in one or more species) can be both ion cyclotron and mirror unstable, the first instability usually dominating over the second one. However, theoretical studies suggest that the addition of a helium component can reduce the ion cyclotron growth rate while leaving the mirror mode instability practically unchanged [Price *et al.*, 1986; Gary, 1993]. Observational studies of the terrestrial magnetosheath support this hypothesis too [Russell and Farris, 1995]. In section 5, we will address this topic.

3.2. Case Study 2: MMS Inside SIR With no Forward Shock

[24] We have found examples of MMS present inside SIRs for which the forward shock has not yet formed. In such cases, MMSs have been usually detected far from the leading edge of the SIR. For instance, on 29 June 2007, STEREO A observed a SIR that started at 11:00 and lasted

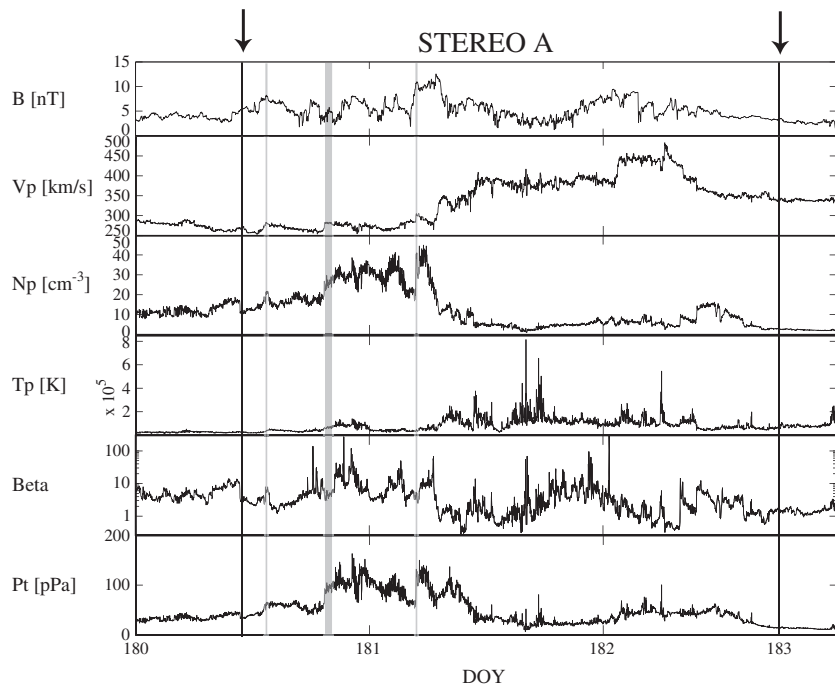


Figure 5. SIR observed from 29 June to 1 July 2008 (edges of SIR are indicated with arrows). Mirror mode storms (shaded area) were observed inside the SIR. The SIR has no forward shock.

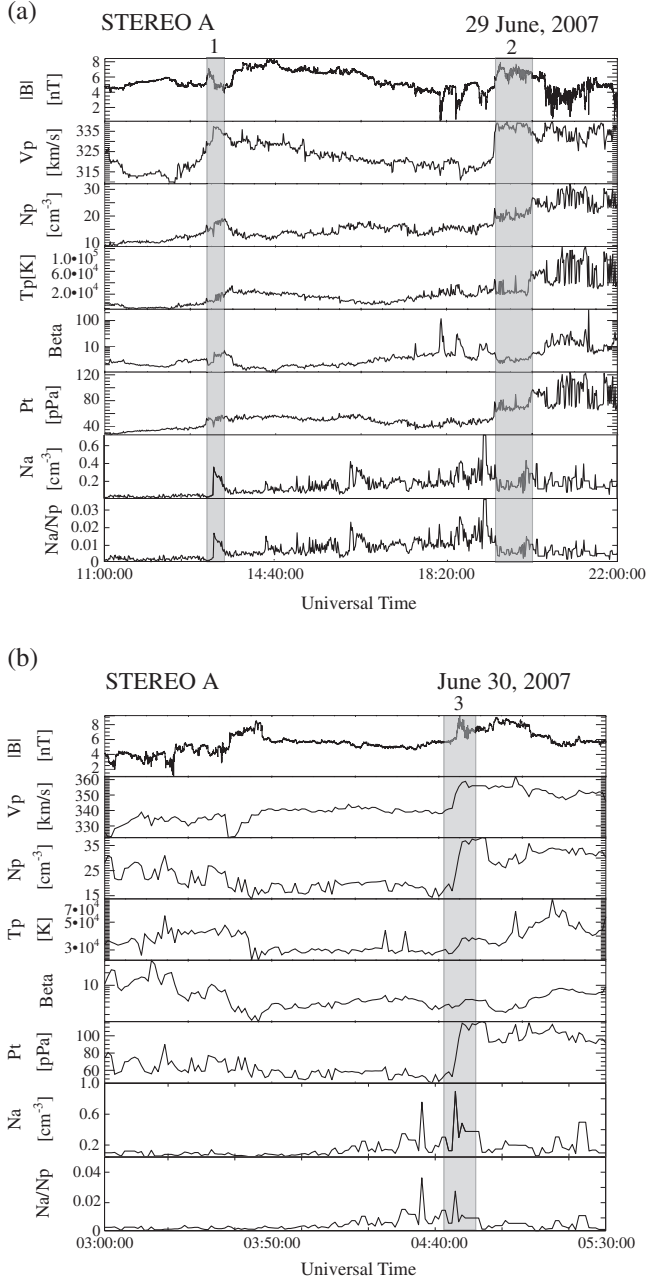


Figure 6. (a) Magnetic field and plasma properties observed near and during two mirror mode storms (shaded areas 1 and 2). Observations are from STEREO A inside the 29 June 2007 SIR. (b) The format is the same as on Figure 6a, except for mirror mode storm 3 (shaded area) observed on 30 June 2007.

until 1 July at 18:00. Figure 5 illustrates magnetic field magnitude and plasma parameters from this SIR. In this case, three MMSs were detected inside the SIR, which are denoted by shaded areas. The first storm was detected on 29 June at 13:10, far from the leading edge of the SIR. Figures 6a and 6b show in more detail the MMS episodes (shaded areas) detected during the SIR: two storms with lengths over 20 min on 29 June (indicated with numbers 1 and 2 in Figure 6a) and one shorter storm on 30 June (see number 3 in Figure 6b). These storms are examples of storms observed far from the leading edge of a SIR. In what

follows, we will analyze plasma properties within these three storms.

[25] The top panels of Figures 6a and 6b show enhancements in plasma velocity and proton number density during the MMs. The same behavior is observed in the total pressure (sum of magnetic pressure and perpendicular plasma thermal pressure). We have found that these features are displayed in most of our MMS events related to SIRs. In contrast, the plasma temperature and the plasma beta do not show important changes when MMs are observed. Mean plasma beta values for storms 1–3 are 4.4, 4.7, and 4.8 respectively.

[26] The last two panels in Figures 6a and 6b provide alpha particle density (N_α) and alpha particle density relative to proton density (N_α/N_p), respectively. It is observed that during the occurrence of storms 1 and 3 (shaded area) mean values of N_α and N_α/N_p are higher than average solar wind values before the storm event. As noted in Figure 6a, the first storm begins on June 29 at 13:10 (far from the initial time of the SIR, registered at 11:00) and coincides with an abrupt increase of N_α , which reaches 5.6 times its value before the storm (see Table 1). Storm 3 shown in Figure 6b starts on June 30 at 04:45:20 and is observed at the same time as a peak in alpha density, here $N_{\alpha 2}/N_{\alpha 1} = 2.7$. For storm 2, there is not an increase in the alpha particle parameters, but they still remain high compared for example to the value of the solar wind registered at the beginning of the SIR, i.e., at 11:00.

[27] Figure 7 shows a close-up of the magnetic field of mirror modes during the storms 1 and 2 observed on 29 June 2007. As in case study 1, mirror-mode structures inside the storm follow an evolutionary pattern. They first appear as small amplitude peaks, which may sometimes grow in amplitude and disappear. Then holes are observed, and by the end of the storm, are very deep. This general trend is also repeated for the storm observed on 30 June 2007, which is not displayed here due to lack of space. Peaks and holes in

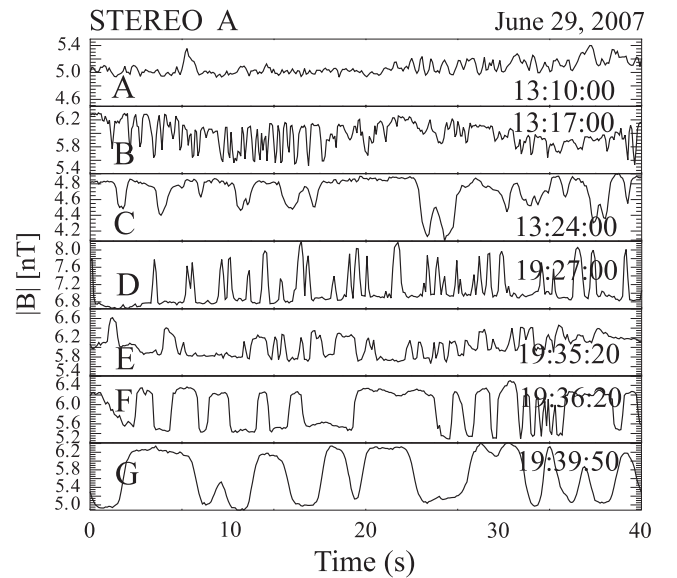


Figure 7. The format is the same as in Figure 4, except for mirror mode storms observed in SIR starting on 29 June 2007.

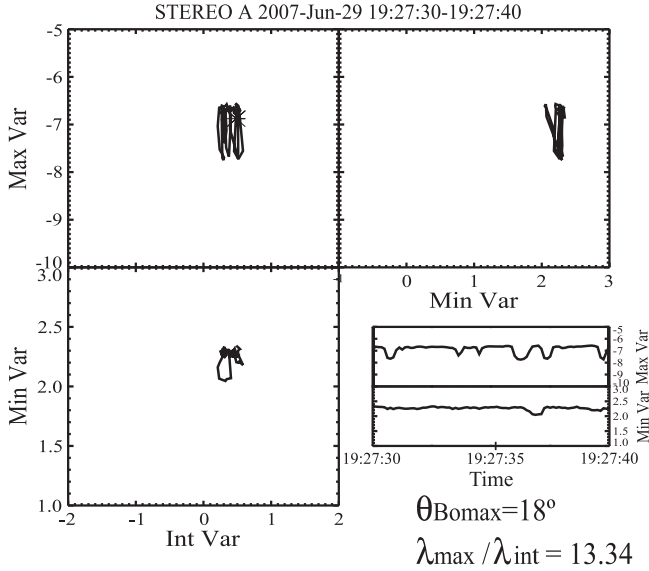


Figure 8. Hodogram derived from MVA for a mirror mode storm observed inside a SIR on 29 June 2007.

this case study display maximum normalized amplitudes around $\delta B/B_0=0.2$.

[28] Figure 8 shows a hodogram derived from MVA for the interval 19:27:20–19:27:40 on 29 June 2007. This figure is a good example of the linear polarization and compressive nature of mirror modes inside storms. In this case $\theta_{max B_0} = 18^\circ$, $\lambda_{max}/\lambda_{int} = 13.34$.

3.3. Case Study 3: MMS in Ambient Solar Wind

[29] We found that MMSs can appear also in the ambient solar wind. Figure 9 shows magnetic field and plasma observations in an interval with ambient solar wind from 07:30 to 08:30 on 29 June 2007. In this case, STEREO B observed a 9 min mirror-mode storm. This example is the only case we found during year 2007 of a mirror-mode storm embedded in pristine solar wind. As seen in Figure 9, the average value of beta is 6.2, which is significantly lower than its value before the storm occurs. As for the alpha particle parameters, the mean value of N_α changed from 0.14 to 0.16 cm^{-3} (i.e., $N_\alpha/N_p=1.2$) and during the storm the mean value of N_α/N_p was 0.017 (see Table 1).

[30] Figure 10 presents the evolution of the storm every 2 min. As can be seen in this figure, the amplitude of the structures does not experience notable changes and is in general smaller than in the SIR cases, i.e., the maximum amplitude during the event reaches $\delta B/B_0=0.18$ approximately. Also, by the end of the event, it is difficult to distinguish if the structures are peaks or holes (see last panel in Figure 10).

[31] Figure 11 shows the results of minimum variance analysis performed for the interval 08:07:21–08:07:37. These waves are linearly polarized because $\lambda_{max}/\lambda_{int} = 47.62$. In this example $\theta_{max B_0} = 3.29$, which means that the analyzed waves have fluctuations almost parallel to the background magnetic field, as expected for mirror-mode waves.

3.4. Summary of Observations

[32] In our 15 month survey, we found more cases of MMSs observed inside SIRs than in the ambient solar wind.

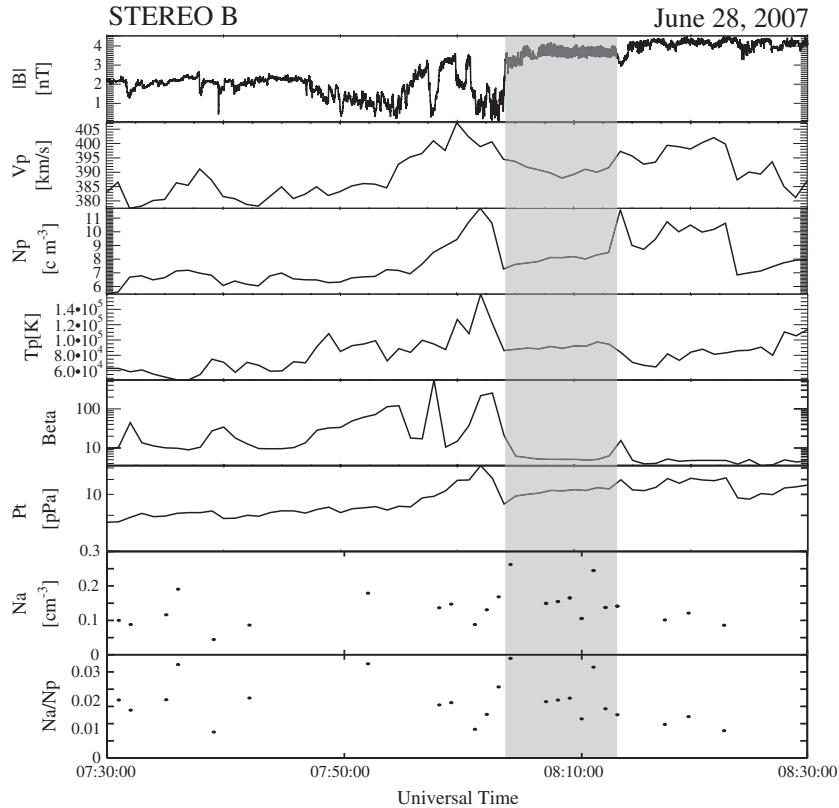


Figure 9. Magnetic field and plasma properties near and during a mirror mode storm (shaded area) observed by STEREO B in the ambient solar wind on 28 June 2007.

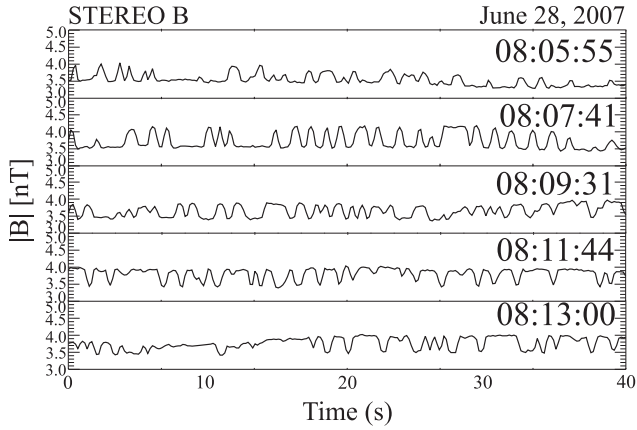


Figure 10. The format is the same as in Figure 4, except for mirror mode storm observed in ambient solar wind on 28 June 2007 by STEREO B.

STEREO A and B observed 40 SIRs between January 2007 and March 2008, and MMSs were found in 11 SIRs, i.e., in almost 30% of the cases. In contrast, we found only one case of an MMS observed in the quiet solar wind.

[33] Most of the storm events associated to SIRs tend to be observed for time intervals ranging from 7 min to 45 min (see Table 1). There is an outstanding event where mirror modes occurred close to the leading edge of a SIR, over an approximately 8 h span. For more details on this latter case, see *Enriquez-Rivera et al.* [2010]. On the other hand, the only case of MMSs found in the ambient solar wind lasted 9 min approximately.

[34] When observed inside the interaction regions, MMSs have been detected near the leading edge of SIRs and also far from it. Interestingly, in all our studied events related to SIRs MMSs have been observed inside the slow solar wind region of the SIR. In Table 1, we calculated the distance (in kilometers) from the leading edge of the SIR using the plasma bulk speed. The mean beta during the storm events is greater than 2, with occasional peaks rising up to values as high as 100. Table 1 shows mean values of the plasma beta for the events observed in 2007 and 2008. Events related with SIRs in which a forward shock was observed in the SIR leading edge are marked with “Y” in Table 1. We will discuss the observed values of beta in the following sections.

[35] Table 1 shows that nearly 70% of the events undergo enhancements of at least 20% in the mean value of the alpha particle density (N_α) compared to its mean value before the mirror-mode storm. The first storm reported in case study 2 is a notorious case where, during the storm, N_α incremented 5.6 times its value before the storm. We also calculated the mean value of the alpha particle density relative to the proton density (N_α/N_p), which ranges between 0.002 and 0.025 (i.e., between 0.2% and 2.5%). The maximum observed value of $N_\alpha/N_p=2.5\%$ was found during a storm observed in the leading edge of a SIR (no forward shock was observed) detected on 26 September 2007 by STEREO B. Because alpha particle enhancements seem to play an important role in the mirror-mode instability, we will discuss this issue in sections 3 and 4.

[36] An important feature of MMSs observed inside SIRs is that their holes and peaks seem to be more nicely shaped

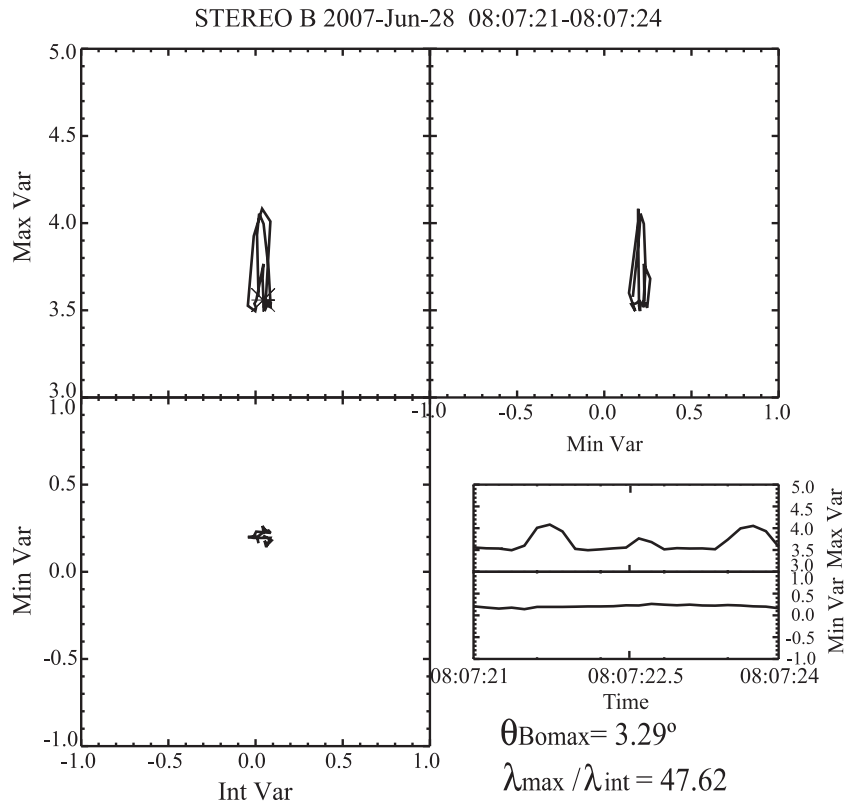


Figure 11. Hodogram derived from MVA in a mirror mode storm observed in ambient solar wind on 28 June 2007.

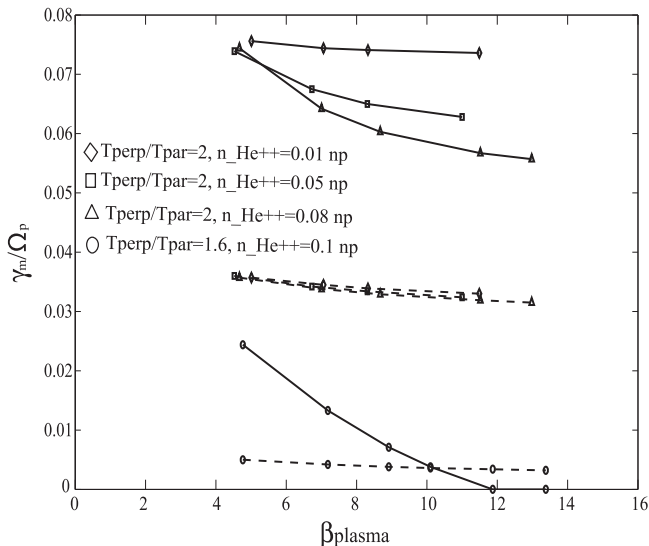


Figure 12. Curves of maximum growth rate (γ_m/Ω_p) versus plasma beta for different anisotropies for ion/cyclotron instability at $\theta_{B_0K} = 0^\circ$ (solid curves) and mirror instability at $\theta_{B_0K} = 65^\circ$ (dashed curves) obtained with input parameters in Table 2.

than in the only case observed in the ambient solar wind. What is more, mirror-mode structures inside interaction regions usually display an evolution from peaks to holes, the latter being wider and deeper as the end of the storm is approached. In contrast, the amplitude of mirror-mode structures in the storm related to ambient solar wind remains practically unchanged and there is not a clear transition between peaks and holes.

[37] Maximum normalized amplitudes ($\delta B/B_0$) of mirror-mode structures in storms related to SIRs range between 0.1 and 0.9. In the ambient solar wind case the maximum amplitude found was 0.18. It is important to note, however, that we need to study more cases of MMSs embedded in the ambient solar wind to see if this behavior is a general trend. Minimum variance analysis in the three case studies did not display significant differences regarding the type of polarization and the value of $\theta_{\max B_0}$. In all cases, there are both elliptically and linearly polarized waves.

4. Kinetic Dispersion Analysis

[38] We use the program WHAMP (Waves in Homogeneous, Anisotropic Multicomponent Plasmas) [Rönmark, 1982] to solve the linear dispersion relation for a plasma with characteristics similar to the plasma where STEREO observed MMSs. The plasma is considered to be homogeneous, magnetized, and collisionless. A three-component, two-ion species plasma is considered with a dense core of protons (denoted by p), a more tenuous population of alpha particles (He⁺⁺, denoted by a) and electrons. The program input parameters are the magnetic field strength, density, temperature of all the species, as well as their temperature anisotropy. All the parameters used as input for the dispersion relation solver are averaged values observed by STEREO from mirror-mode storm events observed in 2007 and 2008, except for the proton temperature anisotropy. Because STEREO has not yet provided temperature

anisotropies (T_\perp/T_\parallel), we assume proton temperature anisotropies between 1 and 3 based on previous solar wind measurements at 1 AU [Winterhalter et al., 1994; Liu et al., 2006; Marsch et al., 1982; Marsch, 1991; Gary et al., 2002].

[39] Linear Vlasov theory predicts that both the ion cyclotron instability and the mirror mode instability can occur in bi-Maxwellian plasmas where the plasma beta is high (beta 1) and temperature anisotropies are moderate-high [Tajiri, 1967; Hasegawa, 1969]. The ion cyclotron instability has a lower threshold anisotropy at intermediate and low beta [Gary et al., 1976; Gary, 1992], which implies that the mirror instability should be observed only above some critical value of beta. However, it has also been noted that the addition of a helium component (i.e., alpha particles) in the plasma introduces damping of the proton cyclotron instability while leaving the mirror-mode unaffected [Price et al., 1976], thereby reducing the critical value of beta. This is in agreement with observational studies of the Earth's magnetosphere. Russell and Farris [1995] showed that at beta values above 3 with an alpha-particle composition of 4%, mirror-mode waves dominate downstream of the Earth's bowshock, possibly because the ion-cyclotron waves are heavily damped.

[40] Figure 12 shows maximum wave growth rates γ_m (normalized by the proton-cyclotron gyrofrequency Ω_p) calculated for the ion cyclotron at $\theta_{B_0K} = 0^\circ$ (solid lines) and the mirror mode instability $\theta_{B_0K} = 65^\circ$ (dashed lines) for plasma beta values between 4 and 14. Curves of growth rates with four different alpha particle densities are shown in the graph. Circles denote the case $Na = 0.1 Np$, triangles are used for $Na = 0.08 Np$, squares indicate $Na = 0.05 Np$, and diamonds are for $Na = 0.01$. These curves were obtained using proton temperature anisotropy values of 1.6 and 2. The alpha particle distribution is considered isotropic, i.e., $T_{a\perp}/T_{a\parallel} = 1$. The plasma values used as input for these curves are shown in Table 2.

[41] We find that both the mirror mode and ion cyclotron instability can grow for plasmas resembling the solar wind at 1 AU. In the cases where alpha particle densities are $Na/Np < 0.09$, approximately, there is a dominance of the ion cyclotron instability over the mirror mode instability at proton temperature anisotropies greater than 2. This is illustrated in the curves with diamonds, squares, and triangles in Figure 12. On the other hand, when $Na/Np > 0.09$ and the anisotropy decreases, growth rates for both instabilities become significantly closer. The latter case is illustrated through the curves with circles in Figure 12. Here the proton temperature anisotropy is 1.6 and the alpha ratio Na/Np is 10%. An interesting feature to note in the curves with circles of Figure 12 is that at $\beta = 10$ approximately, the mirror mode instability starts dominating over the ion cyclotron instability.

Table 2. Input Parameters Used in WHAMP to Obtain Curves in Figure 12

B (nT)	2.7–4.0
Proton temperature (K)	2.8×10^4 – 1.15×10^5
Proton density (cm^{-3})	8.0–20.0
Plasma beta	4.0–14.0
Alpha density (cm^{-3})	0.01–0.1 np
Alpha temperature (K)	1.3×10^5
Proton temp. Anisotropy	1.6 and 2

[42] The results shown in Figure 12 demonstrate that the increase of alpha particle densities relative to the proton density (Na/Np) leads to a decrement of growth rates for both instabilities. Such a decrement is more evident for the ion cyclotron instability, namely, γ_m/Ω_p decreases faster for the ion cyclotron instability than for the mirror instability. In Figure 12, the curves with diamonds, squares, and triangles show that when Na/Np increases from 0.01 (diamonds) to 0.08 (triangles), at a fixed proton temperature anisotropy of 2, the ion cyclotron growth rate (solid lines) experiences a notable decrement, while the mirror instability undergoes a slight decrement (i.e., the diamonds, squares and triangles in dashed lines are very close to each other). This result agrees with previous theoretical studies where it has been suggested that the addition of helium species to mirror/ion-cyclotron unstable plasmas has a greater impact on the ion-cyclotron instability growth rate, which experiences damping. In contrast, the growth rate of the mirror mode instability remains almost unaffected [Price *et al.*, 1986; Gary, 1993].

[43] The curves of wave growth obtained by solving the kinetic dispersion relation have positive wave growth rates within the range of the observed plasma parameters for both the mirror mode instability and the ion cyclotron instability. This is an important result, because it leads to the possibility that some of the mirror-mode structures observed in MMSs might be generated locally via the kinetic mirror mode instability. We further examine this scenario in the following section.

5. Discussion and Conclusions

[44] We have presented three case studies in which mirror-mode waves are observed as MMSs in the solar wind. Case study 1 and case study 2 correspond to MMSs related to SIRs, while case study 3 represents a mirror-mode storm observed in pristine solar wind. Based on our survey, we believe that MMSs are events more commonly observed within SIRs than in the ambient solar wind. A natural question that arises is the reason for this preference.

[45] On one hand, from our 15 events studied in this paper, we found 5 events of MMSs close to the downstream regions of forward shocks preceding SIRs (see Table 1). This suggests that SIR shock regions seem to be suitable environments for the growth of mirror mode instabilities. Here nonuniform plasma shock heating and compression can favor the existence of temperature anisotropies as well as high values of plasma beta. As noted in previous theoretical and observational works, when both parameters are large, the mirror instability occurs. In all the STEREO MMS events observed close to forward shocks of SIRs $\beta > 2.4$ (see Table 1), which is sufficiently high for the mirror-mode instability to occur. Winterhalter *et al.* [1994] observed magnetic holes between 1 and 5.4 AU in sites where the solar wind was unstable to the mirror instability with average plasma betas between 1 and 10. Liu *et al.* [2006] found mirror-mode structures in the sheaths of magnetic clouds preceded by shocks, where the averaged observed value of $\beta_{\perp p} \approx 12$ with values sometimes exceeding 50. Also, previous observational works in the Earth's magnetosheath have reported mirror-mode structures in

regions where the plasma beta is greater than 3 [Russell and Farris, 1995].

[46] Up to this date, STEREO has not yet provided proton temperature anisotropies. In our MMS events close to SIRs' forward shocks, we would expect high temperature anisotropy values near the shock and probably smaller values far from the shock, because enhanced wave particle interaction can lead to isotropization. In our theoretical analysis we found that the plasma is mirror unstable for proton temperature anisotropies between 1.5 and 2 for $4 < \beta < 14$. This range of values found for temperature anisotropies are close to the values found in mirror unstable sheaths from ICMEs analyzed in Liu *et al.* [2006], where the proton temperature anisotropy was enhanced to values of 1.2 and 1.3 for $\beta_{\perp p} \approx 12$. It is also important to bear in mind that the larger the beta, the less anisotropy is required, or in other words, it is the combination of the beta and temperature anisotropy values that plays an important role in making the plasma unstable to the mirror instability.

[47] On the other hand, most of our MMSs (nearly 70%) were found in SIRs where no IP shocks were observed in the nearby region, as shown by case studies 2 and 3. This shows that the existence of an interplanetary shock is not necessary to observe MMSs in the solar wind. Case study 2 shows examples of mirror modes observed inside SIRs far from the leading edge of a SIR where the forward shock has not yet formed, and case study 3 is a mirror-mode storm observed in pristine solar wind with no IP shock detected near the MMS. In these two case studies, the value of beta is greater than 4, as expected for the value of beta in mirror unstable plasmas. As shown in Table 1, average values of beta for the rest of the events studied in this work with no IP shock associated with the SIR range between 2.4 and 32.7. As pointed out in section 2.4, such values of beta are not higher than the values observed in regions surrounding the storm interval. However, according to linear theory, these observed values of beta can make a plasma unstable to the mirror mode instability.

[48] An interesting observation is that the alpha particle density experiences enhancements during most of our mirror-mode storm events. It has been pointed out that the content of alpha-particles plays an important role in mirror unstable plasmas [Price *et al.*, 1976; Gary, 1993; Russell and Farris, 1995]. In the mirror-mode events reported by Liu *et al.* [2006]. The authors studied ICMEs sheaths where $Na/Np > 8\%$. Russell and Farris reported alpha particle content of 4% in magnetospheric regions where mirror modes were observed. In nearly 70% of our MMS events, there are enhancements in the mean alpha particle density (Na), and the mean alpha particle density relative to proton density during the storms is $Na/Np < 2.5\%$. Our results using kinetic linear theory show that for the observed range of Na/Np 2.5% and plasma $\beta < 14$, the mirror mode instability has positive growth rates, i.e., the plasma where MMSs are observed is mirror unstable.

[49] To sum up, there is theoretical and observational evidence that supports the possibility that MMSs observed by STEREO inside SIRs and in ambient solar wind might be generated locally via the mirror mode instability. Nevertheless, there is still another important issue in discussion. For the observed conditions in the solar wind, linear theory

predicts that the ion-cyclotron waves have positive wave growth rates, which are approximately twice the growth rates for the mirror mode. In fact, the dominance of the mirror mode instability over the ion-cyclotron instability in the solar wind occurs when $N\alpha/N\beta > 9\%$ and $\beta > 10$. Although our theoretical value of 9% is very close to that observed in the solar wind by *Liu et al.* [2006], it is still significantly higher than the maximum value of 2.5% observed in our MMS events.

[50] The fact that STEREO observed only MMSs in plasma regions where linear theory predicts that growth rates for this mode are smaller than for the ion-cyclotron instability makes us think that ion-cyclotron waves could be generated together with the mirror mode. In STEREO MMS observations, there are no ion-cyclotron waves present, however. The question that follows now is why the ion-cyclotron waves are not being observed simultaneously with MMSs or in the nearby region. A possible explanation is that because ion-cyclotron waves have phase velocities much greater than the mirror-mode waves, we are not able to observe them in the same region where MMSs are present because they might have left the region of observation. That both waves are cogenerated even when their growth rates are very different was shown observationally by *Russell et al.* [2006] for the low beta conditions in the Saturnian magnetosphere and has also been observed in simulations [*McKean et al.*, 1992, 1994].

[51] At this point, based on our observations of MMSs and on our results from the kinetic study, we can draw partial conclusions as to the origin of MMSs observed in the solar wind. We propose a scenario where MMSs were generated locally in the solar wind where they were observed by STEREO via the mirror mode instability in the same region where ion-cyclotron waves were probably also generated. The difference of phase velocities between both waves could explain the absence of ion-cyclotron waves in STEREO observations. There is also the possibility of the existence of nonlinear phenomena inherent to MMSs, which might result in alterations in the growth rates of the instabilities favoring the growth rate for the mirror mode. Such effects are beyond the scope of our linear approach.

[52] The evolutionary path between peaks and holes in the three case studies presented here is also an interesting feature. No matter how long the storm is, in all cases, mirror-mode structures are observed first as peaks and then as holes. Such peaks tend to grow in amplitude and then are replaced by holes, which may also grow in amplitude and become big holes. This behavior is similar to mirror-mode observations in planetary magnetosheaths such as Earth [*Génot et al.*, 2001], Jupiter [*Bavassano Cattaneo et al.*, 1998; *Joy et al.*, 2006], and Saturn [*Erdős and Balogh*, 1996]. In these environments, mirror-mode peaks are preferentially observed near the planetary shock and in the middle magnetosheath, while holes tend to appear close to the magnetopause.

[53] The formation mechanisms of mirror-mode peaks and their apparent evolution into holes is still a matter of investigation. There are observational studies of planetary environments that emphasize the dependence of mirror-mode shape on the value of β [*Erdős and Balogh*, 1996, *Joy et al.*, 2006]. In these works, peaks (holes) are related to higher (lower) beta plasma conditions than background. In our survey of MMS in the solar wind presented here, we found this

correlation in nearly half of the cases. A case study that shows such correlation is discussed in *Enríquez-Rivera et al.* [2010]. In that study, the authors reported one event observed by STEREO B on 10 July 2007, where MMSs were observed during 8 h approximately. In these MMSs, mirror mode peaks were related to high beta regions while holes were found in different regimes of beta. We also found the presence of magnetic holes in regions where $\beta < 1$, which is not a suitable range value for β in mirror unstable plasmas. The fact that magnetic holes have been observed in both mirror unstable and stable plasma conditions has been suggested to be a signature of bistability [*Génot et al.*, 2009, and references therein].

[54] Other works discuss the mirror-mode evolution from peaks to holes in terms of the distance to mirror threshold. For example, in the context of Saturn's magnetosheath, *Joy et al.* [2006] argued that peaks are a signature of the nonlinear saturation of mirror modes while holes are collapsing structures in a plasma near the linear mirror threshold. Both points of view, dependence of mirror mode shape on β and distance to mirror threshold, are feasible. More simulation work has to be done in this area.

[55] For future work, we will analyze the sheaths associated to fast ICMEs. Because shocks ahead of fast ICMEs usually have high Mach numbers, their sheaths are more perturbed (as in planetary sheaths) and this can lead to plasma instabilities such as the mirror mode instability. ICMEs' sheaths, Earth's magnetosheaths, and SIR geometries all have in common that they are elongated compression regions with the magnetic field tending to lie parallel to their long direction and perpendicular to the compressive force. Therefore, it will be interesting to see if mirror-mode storms occur in ICMEs' sheath regions and compare their characteristics with the storms observed inside SIRs and in the ambient solar wind.

[56] **Acknowledgments.** OER and XBC thank DGAPA/PAPIIT grant 110511-3. Janet Luhmann acknowledges the NASA support of the STEREO project and the IMPACT investigation at the University of California, Berkeley, through grant NAS5-031031.

References

- Bavassano Cattaneo, M. B., C. Basile, G. Moreno, and J. D. Richardson (1998), *J. Geophys. Res.*, *103*, 11961–11972.
- Burlaga, L. F., N. F. Ness and Acuña M. H (2006), Trains of magnetic holes and magnetic humps in the heliosheath, *Geophys. Res. Lett.*, *33*, L21106, doi:10.1029/2006GL027276.
- Enríquez-Rivera, O., X. Blanco-Cano, C. T. Russell, L. K. Jian and J. G. Luhmann (2010), Mirror mode structures in the solar wind: STEREO observations, *AIP Conf. Proc.*, *1216*, 276–279.
- Erdős, G., and A. Balogh (1996), Statistical properties of mirror mode structures observed by Ulysses in the magnetosheath of Jupiter, *J. Geophys. Res.*, *101*, 1–12.
- Galvin, A. B., et al. (2008), The plasma and suprathermal ion composition (PLASTIC) investigation on the STEREO observatories, *Space Sci. Rev.*, *136*, 437–486.
- Gary, S.P. (1992), The mirror and ion cyclotron anisotropy instabilities, *J. Geophys. Res.*, *97*, 8519–8529.
- Gary, S.P. (1993), *Theory of Space Plasma Microinstabilities*, Cambridge University Press, New York.
- Gary, S.P., B. E. Goldstein, and M. Neugebauer (2002), Signatures of wave-ion interactions in the solar wind, *J. Geophys. Res.*, *107*, doi:10.1029/2001JA000269.
- Gary, S. P., M. D. Montgomery, W. C. Feldman, and D. W. Forslund (1976), Proton temperature anisotropy instabilities in the solar wind, *J. Geophys. Res.*, *81*, 1241.

- Génot, V., S. J. Schwartz, C. Mazelle, M. Balikhin, M. Dunlop, and T. M. Bauer (2001), Kinetic study of the mirror mode, *J. Geophys. Res.*, *106*(A10), 21,611–21,622, doi:10.1029/2000JA000457.
- Génot, V., E. Budnik, P. Hellinger, T. Passot, G. Belmont, P. M. Trávníček, P.-L. Sulem, E. Lucek, and I. Dandouras, (2009), Mirror structures above and below the linear instability threshold: Cluster observations, fluid model and hybrid simulations, *Ann. Geophys.*, *27*, 601–615, doi:10.5194/angeo-27-601-2009.
- Hasegawa, A. (1969), Drift mirror instability in the magnetosphere, *Phys. Fluids*, *12*, 2642.
- Jian, L., C. T. Russell, J. G. Luhmann, and R. M. Skoug (2006), Properties of Interplanetary Coronal Mass Ejections at One AU During 1995–2004, *Sol. Phys.*, *239*, 337, doi:10.1007/s11207-006-0132-3.
- Joy, S. P., Kivelson, M. G., Walker, R. J., Khurana, K. K., Russell, C. T., and Paterson, W. R., (2006), Mirror mode structures in the Jovian magnetosheath, *J. Geophys. Res.*, *111*, A12212, doi:10.1029/2006JA011985.
- Krauss-Varban, D., N. Omid, and K. B. Quest (1994), Mode properties of low-frequency waves: Kinetic theory versus Hall-MHD, *J. Geophys. Res.*, *99*(A4), 5987–6009.
- Liu, Y., J. D. Richardson, J. W. Belcher, J. C. Kasper, and R. M. Skoug (2006), Plasma depletion and mirror waves ahead of interplanetary coronal mass ejections, *J. Geophys. Res.*, *111*, A09108, doi:10.1029/2006JA011723.
- Lucek, E. A., M. W. Dunlop, A. Balogh, P. Cargill, W. Baumjohann, E. Georgescu, G. Haerendel, and K.-H. Fornacon (1999), Identification of magnetosheath mirror modes in Equator-S magnetic field data, *Ann. Geophys.*, *17*, 1560–1573.
- McKean, M. E., S. P. Gary, and D. Winske (1992), Mirror and ion cyclotron anisotropy instabilities in the magnetosheath, *J. Geophys. Res.*, *97*, 19,421–19,432.
- McKean, M. E., D. Winske, and S. P. Gary (1994), Two-dimensional simulations of ion anisotropy instabilities in the magnetosheath, *J. Geophys. Res.*, *99*, 11,141–11,153.
- Marsch, E., K.-H. Mühlhauser, R. Schwenn, H. Rosenbauer, W. Pilipp, and F. Neubauer (1982), Solar wind protons: Three dimensional velocity distributions and derived plasma parameters measured between 0.3 and 1 AU, *J. Geophys. Res.*, *87*, 52–72.
- Marsch, E. (1991), Kinetic Physics of the Solar Wind Plasma, in *Physics of the Inner Heliosphere*, edited by R. Schwenn and E. Marsch, Springer-Verlag, Heidelberg, Germany, 45–133.
- Price, C. P., D. W. Swift, and L.-C. Lee (1986), Numerical simulation of nonoscillatory mirror waves at the Earth's magnetosheath, *J. Geophys. Res.*, *91*, 101.
- Russell, C.T., and M. H. Farris (1995), Ultra low frequency waves at the Earth's bow shock, *Advances in Space Research*, *15* (8-9), 285–296.
- Russell, C. T., J. S. Leisner, C. S. Arridge, M. K. Dougherty, and X. Blanco-Cano (2006), Nature of magnetic fluctuations in Saturn's middle magnetosphere, *J. Geophys. Res.*, *111*, A12205, doi:10.1029/2006JA011921.
- Russell, C. T., L. K. Jian, J. G. Luhmann, T. L. Zhang, F. M. Neubauer, R. M. Skoug, X. Blanco-Cano, N. Omid, and M. M. Cowee (2008), Mirror mode waves: Messengers from the coronal heating region, *Geophys. Res. Lett.*, *35*-15, L15101, doi:10.1029/2008GL034096.
- Russell, C. T., X. Blanco-Cano, L. K. Jian, and J. G. Luhmann (2009), Mirror-mode storms: STEREO observations of protracted generation of small amplitude waves, *Geophys. Res. Lett.*, *36*, L05106, doi:10.1029/2008GL037113.
- Rönmark, K. (1982) WHAMP, Kiruna Geophys. Inst. Kiruna, Sweden, Rep. 179.
- Schekochihin, A. A., S. C. Cowley, R. M. Kulsrud, M. S. Rosin, and T. Heinemann (2008), Nonlinear Growth of Firehose and Mirror Fluctuations in Astrophysical Plasmas, *Phys. Rev. Lett.*, *100*, 081301.
- Sonnerup, B. U. O., and M. Scheible, (1998), Analysis Methods for Multi-spacecraft Data. ISSI Scientific Report.
- Southwood, D. J., and M. G. Kivelson, (1993), Mirror instability: I. Physical mechanism of linear instability, *J. Geophys. Res.*, *98*, 9181.
- Tajiri, M. (1967), Propagation of hydromagnetic waves in collisionless plasma., II, Kinetic approach, *J. Phys. Soc. Jpn.*, *22*, 1482.
- Tátrallyay, M., and G. Erdős (2005), Statistical investigation of mirror type magnetic field depressions observed by ISEE-1, *Planetary and Space Science*, *53*(1-3), 33–40.
- Tsurutani, B.T., G. S. Lakhina, D. Winterhalter, J.K. Arballo, C. Galvan, and R. Sukurai (1999), Energetic particle cross-field diffusion: Interaction with Magnetic Decreases (MDs), *Nonlinear Proc. Geophys.*, *6*, 235–242.
- Tsurutani, B.T., D. J. Southwood, E. J. Smith, and A. Balogh, (1992), Non-linear magnetosonic waves and mirror mode structures in the March 1991 Ulysses interplanetary event, *Geophys. Res. Lett.*, *19*, 1267.
- Winterhalter, D., M. Neugebauer, B. E. Goldstein, E. J. Smith, S. J. Bam, and A. Balogh, (1994), Ulysses field and plasma observations of magnetic holes in the solar wind and their relation to mirror mode structures, *J. Geophys. Res.*, *99*, 23, 371.
- Zhang, T. L., et al. (2008), Characteristic size and shape of the mirror mode structures in the solar wind at 0.72 AU, *Geophys. Res. Lett.*, *35*, L10106, doi:2008GeoRL3510106Z.